TRACER TESTS FOR VARIOUS CARBONATE CORES USING X-RAY CT

M. Fourar[1,2], G. Konan[2], C. Fichen[2], E. Rosenberg[2], P. Egermann[2], and R. Lenormand[2]

[1] Ecole des Mines de Nancy
Laboratoire d'Energétique et de Mécanique Théorique et Appliquée
Parc de Saurupt - 54042 Nancy Cedex, France

[2] Institut Français du Pétrole
1 et 4, avenue de Bois Préau, 92852 Rueil Malmaison Cedex, France

This paper was prepared for presentation at the International Symposium of the Society of Core Analysts held in Toronto, Canada, 21-25 August 2005

ABSTRACT

Tracer tests were conducted for various carbonate cores in order to improve the interpretation of dispersion in heterogeneous porous media. The originality of our approach is to calculate the flux of tracer as a function of time at any location along the sample by using the standard mass balance equation and the concentration measured with a X-ray CT. Using this approach, any model for dispersion can be tested as a relationship between the local flux and the local concentration, preventing the problems linked to the integration of transport equations and boundary conditions. The interpretation of the results by the standard approach based on the proportionality between the dispersive flux and the gradient of concentration shows that the dispersion coefficient is not constant and depends on space location. Experimental results are also analyzed by calculating the first and second moments of the flux as function of distance (equivalent to the arrival times). The first moment (mean arrival time) is proportional to the distance from the inlet whereas the standard deviation versus the distance is well described by a power law. The main result of this study is that the standard approach for dispersion cannot be used for heterogeneous samples.

INTRODUCTION

Tracer dispersion is generally used to characterize petroleum, geothermal reservoirs and aquifers. At this scale, the dispersion results mainly from the spatial variability of the permeability. Tracer tests are also used to measure the accessible pore volume of the samples [1] and determine their dispersion coefficients from the effluent production using the standard convection-dispersion equation [2]. However, the real cores and especially carbonate cores might be highly heterogeneous at various scales [3; 4]. Several studies have demonstrated the role of vugs on the tracer response [5; 6]. It has been recognized that large scale heterogeneities can lead to erroneous relative permeabilities, especially when the unsteady state method is used [7; 8], Consequently, tracer tests are often used to discard heterogeneous samples and avoid expensive core flooding [9]. In this paper, we

present experimental results of the displacement of a passive tracer, i.e. which do not affect the fluid viscosity and density, through various carbonate cores using X-ray CT.
We first present measurements and experimental results of the porosity, permeability, and tracer tests for different core samples. Theses results are then analyzed by determining the flux profiles, dispersion coefficients, mean and variance of the arrival time of the tracer front. We show that the classical approach is not able to describe the tracer displacement in the samples.

MEASUREMENTS

Core selections

Several carbonate samples of 38 mm diameter and 80 mm length were selected. Some photographs of theses carbonate cores are presented in Figure 1. The samples are characterized by the presence of oriented shells and fossilized seaweeds. This alters the local porosity, thereby altering the local permeability. As a result, the selected carbonate samples present heterogeneous structure at scales much larger than pore scales which might affect flow and tracer characterization of core samples. In order to study the impacts of the heterogeneities, experimental measurements of porosity, permeability and dispersion were performed for each sample. In this paper, we present the results obtained with six samples labelled from 1 to 6.

Porosity

Porosity ϕ was measured by using a Hispeed FX/i medical scanner (General Electric). Each core was scanned under two different states: fully saturated with air (fluid 1), and fully saturated with water (fluid 2). The measured CT in each case is the sum of the CT of the porous matrix CT_{pm} and the CT of the fluid CT_{fluid} weighted by the porosity:

$$CT_1 = (1-\phi)CT_{pm} + \phi CT_{fluid\,1} \tag{1}$$

$$CT_2 = (1-\phi)CT_{pm} + \phi CT_{fluid\,2} \tag{2}$$

Eliminating the CT of the porous matrix between the two previous equations one obtains:

$$\phi = \frac{CT_1 - CT_2}{CT_{fluid\,1} - CT_{fluid\,2}} \tag{3}$$

Gas single-phase flow

Permeability K and inertial coefficient β of the samples were deduced from gas (N2) single-phase flow experiments. For each sample, the gas was injected in the core at a constant flow rate and the pressures at the inlet and the outlet of the core were measured. Then, the gas flow rate was increased stepwise within a range where the inertial effect is not negligible. It is important to note that the applied pressure at the outlet was high enough (10 bars) in order to avoid Klinkenberg effects [10]. Under the above conditions,

the flow is governed by the Forchheimer equation [11] written for an incompressible fluid:

$$\frac{P_i^2 - P_o^2}{2P_o L} = \frac{\mu}{K}\frac{Q_o}{A} + \beta\rho_o \frac{Q_o^2}{A^2} \quad (4)$$

where P_i and P_o are pressures at the inlet and the outlet of the sample, Q_o is the volumetric flow rate measured at P_o, μ and ρ_o are the dynamic viscosity and the density (at pressure P_o), L and A are the length and the section area of the sample. Permeability K and inertial coefficient β are dependent on the porous medium structure.

Tracer tests

Tracer test experiments were performed by using two solutions of KI with concentrations of 10 g/l and 150 g/l. For each experiment, the core was initially saturated with a solution of a given concentration. Then, the second solution was injected at a constant rate to displace the solution previously in place. The variation of the tracer concentration was determined from X-ray CT measurements at 16 cross sections of 1 mm thickness located at each 4 mm. As the scanner resolution is 512 mm x 512 mm, the voxel dimension is then 0.12 mm x 0.12 mm x 1 mm. In addition, the variation of the flux of tracer at the outlet was derived from the measurement of the effluent concentration using a conductimeter.

Four different experiments were conducted for each sample:

1 - Displacement of the 10 g/l brine by 150 g/l brine at 100 cc/h (= 1.78 10^{-8} m^3/s);
2 - Displacement of the 150 g/l brine by 10 g/l brine at 100 cc/h (= 1.78 10^{-8} m^3/s);
3 - Displacement of the 10 g/l brine by 150 g/l brine at 200 cc/h (= 5.56 10^{-8} m^3/s);
4 - Displacement of the 150 g/l brine by 10 g/l brine at 200 cc/h (= 5.56 10^{-8} m^3/s).

EXPERIMENTAL RESULTS

Porosity maps

Figure 2 displays four CT scan porosity cross-section images of the sample 1 each 16 mm. Zones of high porosity appear red while zones of low porosity appear blue. These images show clearly that the sample porosity is heterogeneous for each section. Therefore, a 3D scan porosity image of the sample 1 and the corresponding porosity distribution are presented in Figure 3. It appears that the sample porosity is also heterogeneous at the core scale. On the other hand, the heterogeneity of the examined samples is illustrated by the porosity profiles along each core in Figure 4. Values of the mean porosities of all samples are presented in Table 1. They vary between 27 % and 40 %.

Permeability

Experimental measurement results during gas single-phase flow show that the pressure term $\left(P_i^2 - P_o^2\right)/\left(2P_oL\right)$ is a quadratic function of the flow rate Q_o. It must be recalled that this behaviour characterizes the inertia effects due to high flow rates. Values of K and β determined from the parabola in accordance with Equation (3) are presented in Table 1 for all samples. In this paper, we will not study the relationship between heterogeneity and inertial factor.

Table 1 – Experimental values of the porosity, permeability, inertial coefficient, and power law coefficients of the variance of arrival time.

Sample	ϕ (%)	K (mDarcy)	β (10^8 m^{-1})	a	b
1	32	855	2.2	0.12	1.002
2	31	720	1.9	0.36	1.22
3	33	2500	1.3	0.42	1.36
4	30	315	4.1	0.4	0.82
5	27	155	9.5	0.78	1.05
6	40	56	62	6.32	1.27

Concentration profiles

X-ray scan images of the tracer displacement through the sample 1 are shown in Figure 5. They correspond to three cross sections located at different positions from the core inlet (4 mm, 12 mm, and 20 mm) and at different time steps after the beginning of the injection (90 s, 180 s, 280 s, and 380 s). A 3D image of the tracer displacement through the sample 1 is also presented in Figure 6. These images show clearly the tracer front dispersion. As a consequence of the heterogeneity of the porosity, the tracer is also dispersed within each cross section. Comparison between X-ray scan images of the porosity and tracer displacement shows that there is a link between the porosity distribution and the tracer dispersion. However, comparison between Figure 3 and Figure 6 shows that for the tracer reaches the zones of high porosity, it is necessary that these zones might be connected to the inlet of the sample. This indicates that the local permeability must play a critical role in the dispersion processes.

Figure 7 shows the average dimensionless concentration along sample 1 as function of the pore volume injected for different cross sections. For the sake of clarity we represent only a comparison between experimental results obtained during experiments 1 and 2. It can be seen that the curves are almost the same. This is also the case for the results obtained with the other experiments. The concentration profiles do not depend on flow rate and brine concentration. This is a proof that molecular diffusion is negligible. This point is fundamental in our result analysis presented below.

In addition, measurements of the tracer flux at the outlet are presented in Figure 8. The results confirm that there is no influence of the flow rate (100 cc/h and 200 cc/h) neither

of the brine concentration (10 g/l and 150 g/l). We have verified that the fluxes at the outlet are the same for the four experiments conducted with the sample 1. These results also suggest that a dead-end pore model, which has been proposed earlier to analyse tracer tests conducted on heterogeneous samples [4], is not adapted to interpret the experimental data. Because this approach is based on the partition of the porous medium into a flowing and a non-flowing fraction and a coupling term between these two parts (diffusion like exchange coefficient), the experimental results should have been sensitive to the flow rate (time to perform the experiment), which was not observed experimentally.
We have also checked the total mass balance of tracer at the scale of the whole core using the injected mass of tracer (controlled by the pump), the effluent mass (conductimeter) and the local concentration (X-ray).

ANALYSIS OF THE TRACER TEST DATA

Flux profiles

The in-situ concentration measurements performed at close time intervals allow the calculation of the flux of tracer at different cross sections using the mass balance equation, which can be written in a dimensionless form as follows:

$$\frac{\partial C}{\partial t} + \frac{\partial f}{\partial x} = 0 \tag{5}$$

The dimensionless longitudinal coordinate is defined by choosing the length of the sample as the characteristic length. The dimensionless time is defined by choosing the time to completely saturate the sample as the characteristic time. A similar calculation of the flux (or flow rate) using the local saturation have been presented for determining the relative permeabilities in the case of heterogeneous core samples [12]

The results obtained during the four experiments conducted with the sample 1 are shown in Figure 9. For clarity, only some curves of flux are plotted. The superposition of the curves determined from the four experiments confirms that the flow rate and the brine concentration do not have any impact on the displacement mechanism.

Spatial dependence of the dispersion coefficient

Modelling tracer displacement through homogeneous porous media is based on the convection-dispersion equation, which results from the combination of the mass balance equation and the relationship between flux and concentration derived from Fick's law [2]. In dimensionless form this relationship is written as:

$$f = C - D\frac{\partial C}{\partial x} \tag{6}$$

where f is the flux, C is the concentration, x is the longitudinal coordinate, and D is the dimensionless dispersion coefficient. As a consequence of the definitions of the characteristics length and time, the dimensionless dispersion coefficient D is given by:

$$D = \frac{D'}{V\,L} \tag{7}$$

where D' is the dispersion coefficient and V is the front velocity (the flow rate per section area divided by the mean porosity), and L is the core length.

Values of D were calculated for different cross sections along each core using Equation (6), the flux values calculated from in-situ measurements of the concentration by using the mass balance equation, and the gradient of concentration. The calculated values of D vary along the core (Figure 10). The spatial dependence of the dispersion coefficient is the signature of the samples heterogeneity. This confirms that the classical approach is not suitable for modelling tracer displacements in heterogeneous porous media.

This method of determining the dispersion coefficient directly on the differential relationship between the flux and concentration avoid the problem of averaging when the integrated solution is used. In addition, the standard boundary conditions of concentration equal to unity at inlet and semi-infinite medium [9] is questionable.

First and second temporal moment calculations

Through the lack of theoretical models to describe non-Fickian displacements in heterogeneous porous media, it is possible to characterize them by calculating the first and second temporal moments. For a continuous tracer injection, the dimensionless first temporal moment, which represents the mean arrival time of the tracer, is defined by [13]:

$$< t > = \int_0^\infty t\,\frac{\partial F}{\partial t}\,dt \tag{8}$$

The plot of $< t >$ as function of the dimensionless position x is presented in Figure 11. The main result is that the mean arrival time of the tracer front is almost equal to the distance from the inlet of the core for all the examined samples. This result proves that the porosity is uniform along the sample.

The second temporal moment defined by:

$$< t^2 > = \int_0^\infty t^2\,\frac{\partial F}{\partial t}\,dt \tag{9}$$

leads to the variance of the arrival time of the tracer front:

$$\sigma_t^2 = < t^2 > - < t >^2 \tag{10}$$

The plot of σ_t^2 as function of x is presented in Figure 12. The variance at the same distance from the inlet of the core depend on the sample and, consequently, on the heterogeneity. The value of σ_t^2 quantify the degree of the heterogeneity.

Several attempts were made to establish the relationship between the variance of the arrival time of the tracer and the distance from the inlet of the cores. As shown in Figure 12, the power law seems to be appropriate:

$$\sigma_t^2 = a\, x^b \tag{11}$$

Values of a and b for the various samples are presented in Table 1. At this stage, we are not able to determine the dependence of the power law coefficients a and b on other mean properties of the samples (porosity, permeability, inertial coefficient). However, the first results of numerical simulations carried out at present show that the correlation length of the permeability distribution of the sample is one of relevant parameters for determining a and b.

A similar result of power law variances have been proposed for probabilistic approaches of tracer dispersion in porous media [14]. For standard dispersion, an exponent of 1 is observed and for a perfectly layered medium, variance is proportional to the square of the distance.

If we examine the sample 1, there is a contradiction between the interpretation in term of moment that leads to a variance exponent close to 1, signature of a standard dispersion behavior and the results of local dispersion showing a non constant dispersion coefficient. So far, we have no explanation.

CONCLUSIONS

Several carbonates cores were characterized by determining their porosity and permeability. The porosity was measured by using X-ray CT and tracer tests were conducted on theses cores by using X-ray CT to measure in-situ concentrations.

The analysis of the experimental results leads to the following conclusions:

- The mean values of porosity and permeability vary within large intervals;
- The molecular diffusion is negligible in our experiment;
- The dispersion coefficient is space dependent that is the classical approach (Fickian) is not suitable for describing the tracer tests;
- The mean arrival time of the tracer front is proportional to the distance from the inlet of the cores;
- The variance of the arrival time is a power law of the distance.

REFERENCES

[1] Hashemi, S. M., Kazemzadeh, E.-A. and Esfahani, M. R.: Determination of accessible pore volumes of a porous media during miscible displacement using tracer analysis technique", SCA paper 2003-64, Pau, France, 2003

[2] Bear, J., "Dynamics of fluids in porous media", Elsevier, New York , 1972

[3] Siddiqui, S., Funk, J. and Khamees, A.: "Static and dynamic measurements of resevoir heterogeneities in carbonate reservoirs", SCA paper 2000-06, Abu Dhabi, UAE, 2000.
[4] Hidajat I., Mohanty K.K., Flaum M., and Hirasaki G.: Study of Vuggy Carbonates Using NMR and X-Ray CT Scanning. SPE Reservoir Evaluation & Engineering, October 2004.
[5] Moctezuma-B., A. and Fleury, M.: Permeability mapping on vuggy core sample using tracer experiments and streamline simulations", SCA paper 9919, Golden, USA, 1999.
[6] Olivier, P., Cantegrel, L., Laveissière, J. and Guillonneau, N.: Multiphase flow behaviour in vugular carbonates using X-Ray CT, SCA paper 2004-13, Abu Dhabi, UAE, 2004.
[7] Hamon, G. and Roy, C.:"Influence of heterogeneity, wettability and coreflood design on relative permeability curves", SCA paper 2000-23, Abu Dhabi, UAE, 2000
[8] Fenwick, D., Doerler, N. and Lenormand, R.:"The effect of heterogeneity on unsteady-state displacements", SCA paper 2000-25, Abu Dhabi, UAE, 2000.
[9] Dauba, C., Hamon, G., Quintard, M. and Cherblanc, F.: "Identification of parallel heterogeneities with miscible displacement", SCA paper 9933, Golden, USA,1999.
[10] Klinkenberg L., 1951, Bull.GeoL.Soc.AM., 62, pp. 559.
[11] Forchheimer, P. 1901, Wasserberwegung durch Boden. Z. Vereines deutscher Ing. 45 (50), 1782-1788.
[12] Egermann, P. and Lenormand, R.: "A new methodology to evaluate the impact of the local heterogeneity on petrophysical parameters(Kr, Pc): application on carbonate rocks", SCA paper A18, Abu Dhabi, UAE, 2004.
[13] Lenormand, R.:"Determining Flow Equations from Stochastic Properties of a Permeability Field", SPE Journal, Vol. 1, june 1996.
[14] Berkowitz, B. and Scher, H.: "The role of probalilistic approaches to transport theory in heterogeneous media", transport in Porous Media,vol. 42, pp. 241-263, 2001.

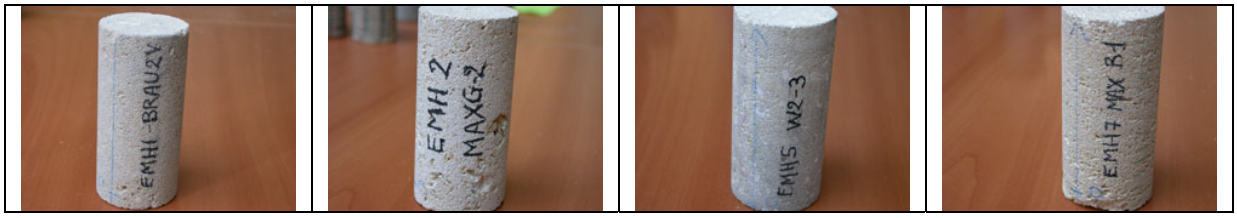

Figure 1 – Photographs of some carbonate cores used for tracer tests.

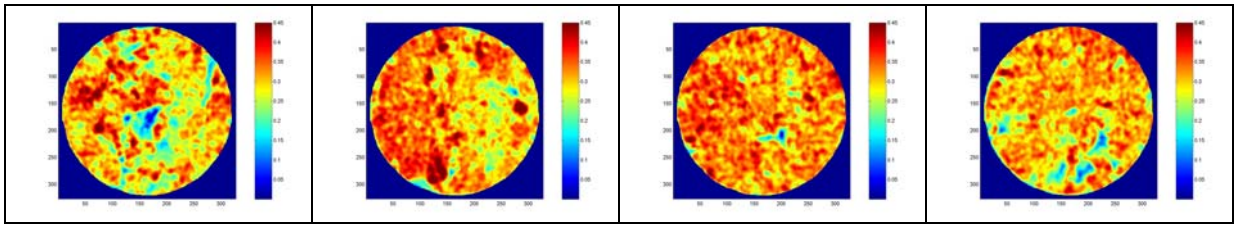

Figure 2 – CT scan porosity images along the sample 1 at regular intervals of 16 mm.

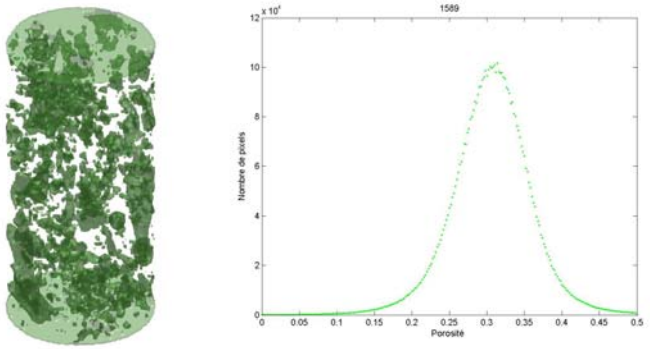

Figure 3 – 3D CT scan porosity image of the sample 1 and the corresponding porosity distribution determined from CT scan measurements.

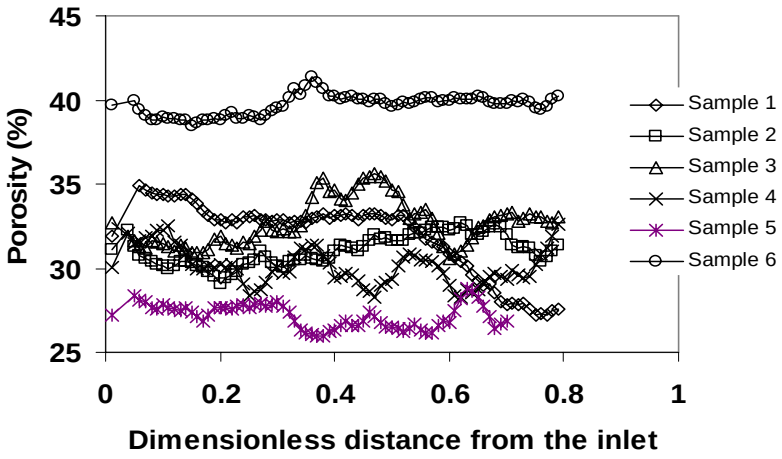

Figure 4 – Porosity profiles along each examined core.

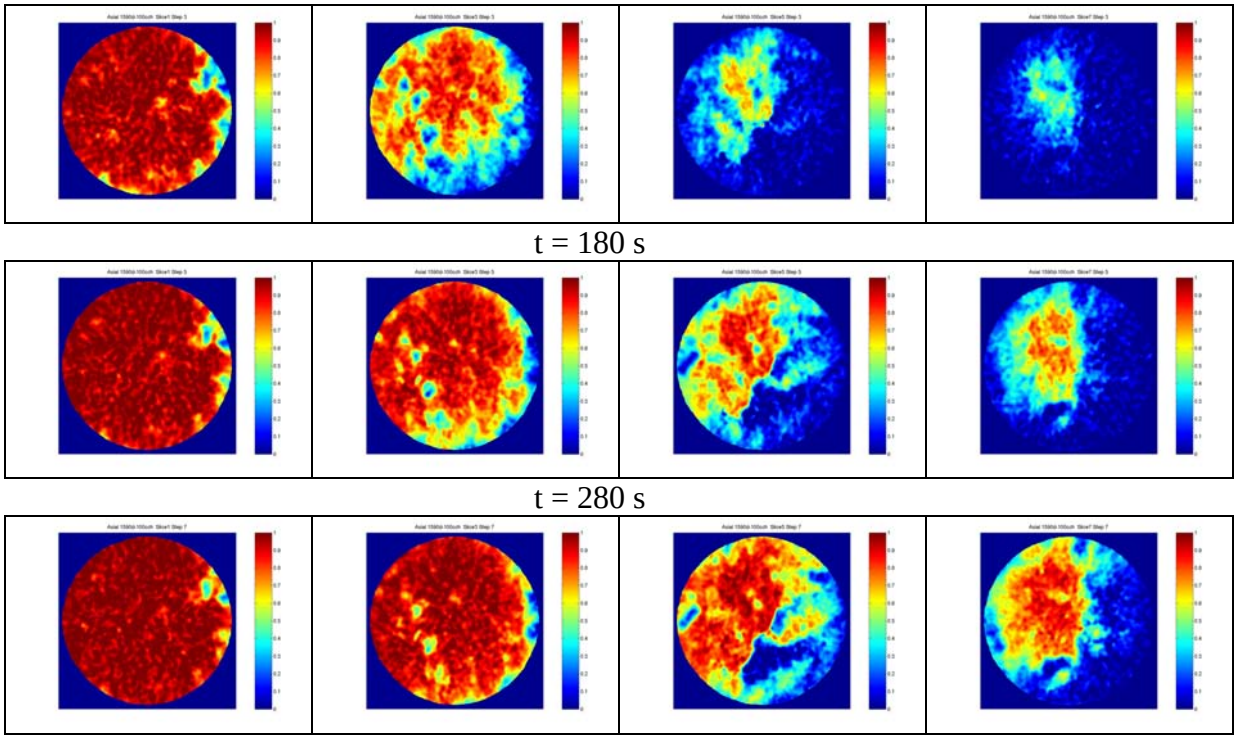

t = 180 s

t = 280 s

t = 380 s

Figure 5 – X-ray scan images of the tracer displacement through the sample 1 for different time steps after the tracer injection. The cross sections are located at 4 mm, 12 mm, and 20 mm from the core inlet.

Figure 6 – 3D scan image of the tracer displacement through the sample 1.

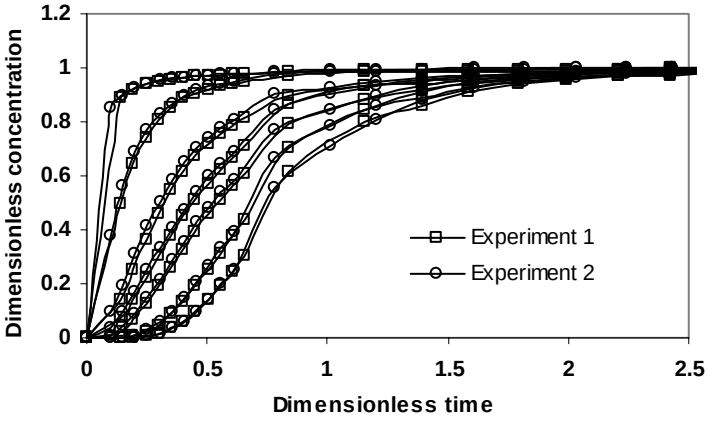

Figure 7 – Average dimensionless tracer concentration as function of time and distance.

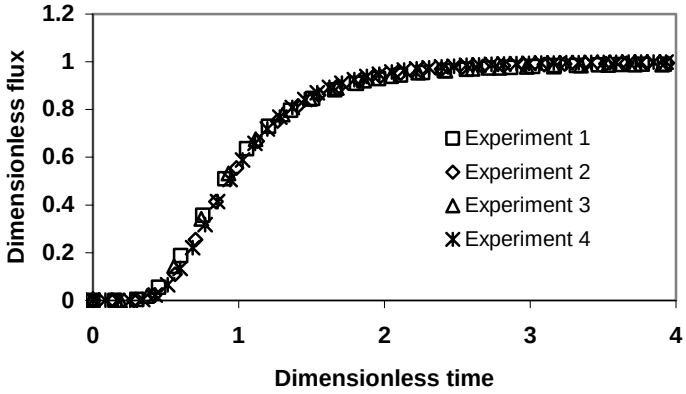

Figure 8 – Dimensionless tracer flux at the outlet of the sample 1.

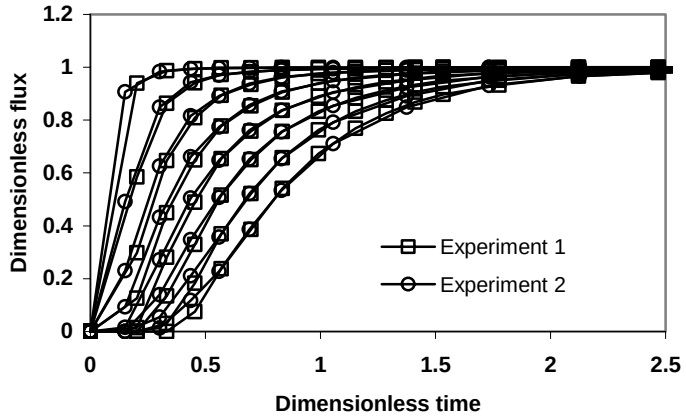

Figure 9 – Dimensionless tracer flux as function of time at different cross sections along sample 1 for two experiments.

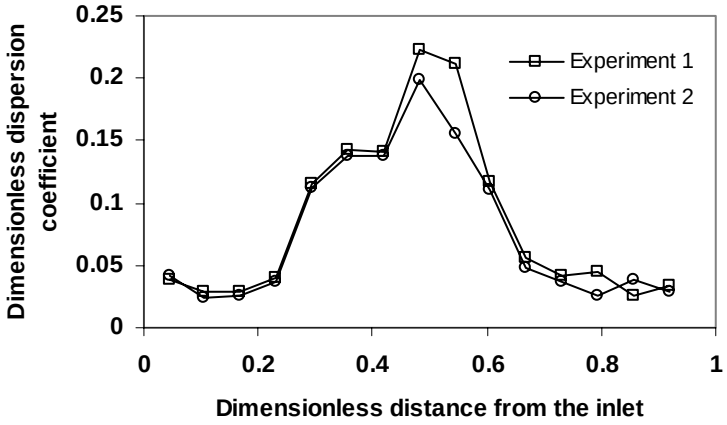

Figure 10 – Dimensionless dispersion coefficient along sample 1 for two experiments.

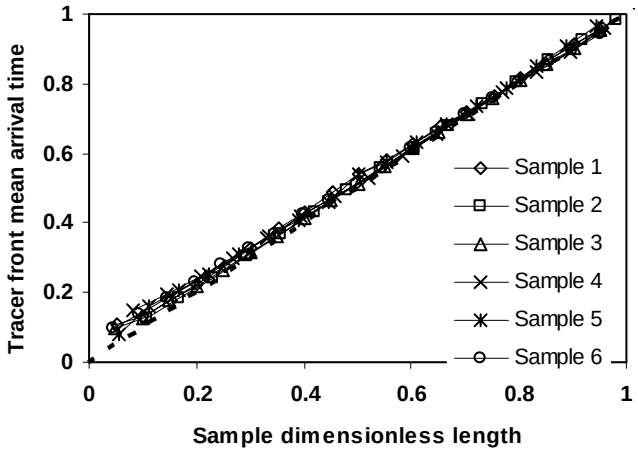

Figure 11 – Tracer front mean arrival time as function of the dimensionless distance from the core inlet

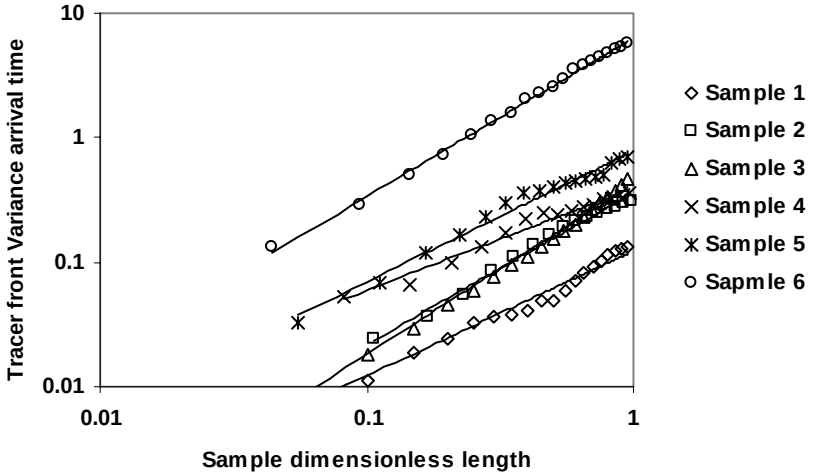

Figure 12–Variance of the tracer front arrival time as function of the dimensionless distance from the core inlet